

PFC/JA-93-34

Particle Dynamics in Chirped-Frequency Fluctuations

C. T. Hsu, C. Z. Cheng,¹ P. Helander,²
D. J. Sigmar, R. White¹

MIT Plasma Fusion Center
Cambridge, Massachusetts 02139 USA

December 1993

¹Permanent address: Princeton Plasma Physics Laboratory, Princeton University, Princeton, NJ 08543

²Permanent address: Institute for Electromagnetic Field Theory and Plasma Physics, Chalmers University of Technology, S-412 96 Göteborg, Sweden

This work was supported by the US Department of Energy under contract DE-FG02-91ER-54109. Reproduction, translation, publication, use, and disposal, in whole or in part, by or for the US Government is permitted.

Submitted for publication in: Physical Review Letters

Particle Dynamics In Chirped-Frequency Fluctuations

C. T. Hsu, C.Z. Cheng^{a)}, P. Helander^{b)},

D.J. Sigmar , and R. White^{a)}

Massachusetts Institute of Technology

Plasma Fusion Center

167 Albany Street, NW16-260

Cambridge, Massachusetts 02139

Hamiltonian systems describing particle motion in a wave with time-dependent (chirped) frequency are studied. The wave is found to form a single-node separatrix (**bucket**) moving in the phase space at a rate proportional to that of the frequency change. Particles trapped inside the bucket undergo convection, while untrapped particles colliding with the bucket get a resonant kick, in phase space. In toroidal systems, these effects can result in a large radial convective flux roughly proportional to the size of bucket and the frequency chirping. Possible applications of this novel mechanism to tokamak plasmas are discussed.

PACS numbers: 03.20.+i, 52.20.Dq

^{a)} Permanent address: Princeton Plasma Physics Laboratory, Princeton University, Princeton, New Jersey 08543.

^{b)} Permanent address: Institute for Electromagnetic Field Theory and Plasma Physics, Chalmers University of Technology, S-412 96 Göteborg, Sweden.

A common characteristic of an evolving nonlinear system is that the wave frequency excited in the system also evolves in time. Such behavior, referred to as frequency chirping [1], can be found in, nonlinear optics [1], developing turbulent systems, and unsaturated systems with nonlinear wave-wave and/or wave-particle interaction. In particular, beam driven activities in tokamak plasmas, especially instabilities with bursting behavior such as *fishbone* oscillations [2], usually exhibit strong frequency chirping. Yet, most particle transport studies carried out so far are based upon the interaction of particles with constant frequency fluctuations. It is therefore worthwhile to study particle dynamics in a chirped frequency fluctuation, i.e., in an accelerating (or decelerating) wave.

First, let us consider the one-dimensional (1-D) Hamiltonian system

$$H = p^2/2 + A(1 - \cos(q - \phi(t))), \quad (1)$$

where ϕ is the wave phase, so that $\dot{\phi}$ is wave frequency, $\ddot{\phi}$ is the frequency chirping, and the amplitude A is assumed to be constant. Note that this Hamiltonian system has been extensively studied [3] in the limit of small frequency chirping $\ddot{\phi} \ll 1$, in which the adiabatic invariant is preserved except for particles very close to the separatrix. In contrast, $\ddot{\phi}$ is allowed to be finite in the present study.

Particle motion in this Hamiltonian system is most easily described in the wave frame, in which $Q \equiv q - \phi(t)$ and $P \equiv p - \dot{\phi}(t)$. The evolution of P and Q is governed by a new Hamiltonian $\hat{H} = P^2/2 + V(Q)$ with the potential $V(Q) \equiv A(1 - \cos Q) + \ddot{\phi}Q$ equivalent to that of a pendulum subject to a drag force $\ddot{\phi}$ along Q . We shall hereby assume that $\ddot{\phi}$ is constant so that both $V(Q)$, as shown in Fig. 1a, and \hat{H} become independent of time. This time-independent Hamiltonian is similar to the one governing electron motion near the synchronous energy in Free Electron Lasers (FEL) [4], where the average slope of $V(Q)$ is induced by the synchronous phase instead of the frequency chirping.

The particle trajectories in P, Q space, illustrated in Fig. 1b, coincide with contours of constant \hat{H} . With this in mind, it is straightforward to observe from Figs. 1a, 1b that

- (i) A single-node separatrix is formed and divides the phase space into two regions: a trapped region inside and an untrapped region outside; this separatrix does not occupy

the whole Q space but leaves an open gap connecting the positive and negative P spaces (see Fig. 1);

- (ii) The action $\oint PdQ$ is invariant for trapped particles;
- (iii) Both $\langle P \rangle$ and $\langle Q \rangle$ are constant for particles trapped in the potential well, where, $\langle \dots \rangle$ indicates an average taken between two neighboring local maxima of P ;
- (iv) $\frac{d}{dt} \langle P \rangle = -\ddot{\phi}$ for passing particles far from the separatrix.

Transforming to the lab frame, one finds that this single-node separatrix is moving in the p -direction at a rate $\frac{d}{dt}p = \ddot{\phi}$. Particles initially loaded inside the separatrix will always be trapped in it and will be dragged along with it in phase space (see Fig. 2a). It is therefore appropriate to refer this convecting separatrix as a "bucket" [4]. The size of the bucket is determined by the action along the separatrix in P, Q space which can be written as

$$S_b(A, \ddot{\phi}) = 8\sqrt{A} \int_0^{\pi-(y_1+y_2)/2} dy \sqrt{\sin y \sin(y+y_1) - \alpha y}. \quad (2)$$

Here $\alpha \equiv |\frac{\ddot{\phi}}{A}|$, $y_1 = \arcsin \alpha$, and y_2 satisfies $\cos y_1 - \cos y_2 = \alpha(2\pi - y_1 - y_2)$. It is evident that S_b decreases with α and vanishes when $\alpha \geq 1$. For $\alpha \ll 1$ $S_b \simeq 16\sqrt{A} (1 + \frac{\pi\alpha}{4} \ln \alpha)$.

For passing orbits reasonably far away from the bucket, $\langle p \rangle$ remains constant. As shown in Fig. 2b however, when the bucket approaches a passing orbit, the p modulation of the orbit increases until it hits the resonance and decelerates (accelerates if $\ddot{\phi}$ is negative) along the rim of bucket and "slides" over to the other side. Then, the bucket moves away from it and $\langle p \rangle$ becomes constant again. It should be noted here that the reason why the passing orbits are allowed to slide through the resonant surface without undergoing separatrix crossing is that the bucket does not occupy the entire Q space, as shown in Fig. 1b, but leaves a gap open. This process causes $\langle p \rangle$ to increase for particles interacting with a decelerating wave ($\ddot{\phi} < 0$) and to decrease when interacting with an accelerating wave ($\ddot{\phi} > 0$). Since this change occurs within just a few bounce periods, the orbit effectively gets a resonant "kick" in momentum space.

Upon noticing the symmetry property with respect to the $P = 0$ axis in P, Q space, one finds that the kick's magnitude is determined by

$$\Delta p = -2\sqrt{A}\sigma_\phi \int_0^{y_1} dy \frac{\sin(2y+y_0)}{G(y)}. \quad (3)$$

Here, $G(y) \equiv \sqrt{\frac{P_0^2}{4A} - \sin y \sin(y + y_0) - \alpha y}$, $\sigma_\phi \equiv \frac{\ddot{\phi}}{|\dot{\phi}|}$, P_0, Q_0 are the initial phase space coordinates, $y_0 \equiv \sigma_\phi Q_0$, and y_1 satisfies $G(y_1) = 0$. This kick decreases with increasing α and actually vanishes when $\alpha \gg 1$. It was previously estimated for the case $\alpha \ll 1$ by using the adiabatic invariant [3,5,6] property of orbits outside the separatrix. In that limit, the particle is considered to undergo separatrix crossing [3] and gets a kick $\Delta p \simeq \frac{8}{\pi} \sqrt{A}$.

In summary, a chirped wave forms a moving bucket if the frequency chirping is smaller than the wave amplitude. The bucket occupies the phase space of size S_b , given in Eq. (2), and transports trapped particles convectively in phase space at the rate of the frequency chirping $\ddot{\phi}$. In other words, the centers of the islands of trapped particle trajectories move at the phase velocity of the wave and therefore stay in resonance. This results in a transport flux in velocity space proportional to $\ddot{\phi} S_b$, which is roughly proportional $\ddot{\phi} \sqrt{A}$. Even for a non-adiabatic change of the frequency (i.e., a finite frequency chirping) there exist adiabatic invariants for most of the phase space except for the passing region near the bucket, while passing particles colliding with the bucket get a resonant kick Δp quantified in Eq. (3). If the frequency chirping is larger than the wave amplitude, the bucket vanishes and no particles are trapped. In this case, most orbits remain unaffected by the wave until they collide with the moving resonance surface and get a momentum kick.

The above conclusions are surprisingly well preserved even when $\ddot{\phi}$ is not constant, as shown in Fig. 2c, where a particle is trapped in a wave with the phase $\phi(t) = t \exp(-t/20)$ and $\langle p \rangle \simeq \dot{\phi} = (1 - \frac{t}{20}) \exp(-t/20)$ is shown to hold. However, it should be noted that even though the amplitude is constant, the evolution of $\ddot{\phi}$ causes a change of the bucket size according to Eq. (2). This results in separatrix crossings of particle orbits into or out of the bucket, according to Liouville's theorem, in the same way as in a system with non-constant amplitude. If there exist two buckets moving at different speeds in the phase space, a locally stochastic region forms when they collide. After the collision, they depart from each other, and each one carries some particles with it. A particle originally in one bucket can then end up in the other bucket after the collision. A detailed discussion of these more complex features of particle dynamics in chirped waves as well as more detailed calculations of the phenomena presented here will be given in a separate paper [7].

In a system with many degrees of freedom, it is wellknown [6,8,9] that, as long as the perturbed Hamiltonian is sufficiently small so that the coupling between two neighboring resonant surfaces is negligible, the 1-D Hamiltonian faithfully reproduces the behavior of the multi-dimensional system. Therefore, the effects of frequency chirping are at least qualitatively similar for the two systems. In particular, they both can form buckets moving with the resonant islands. In a toroidally confined axisymmetric plasma, the guiding center motion of charged particles is governed by the following Hamiltonian [10]

$$H = \frac{1}{2M} \left(P_\zeta + \frac{Ze}{c} (\psi_p - \tilde{A}_\zeta) \right)^2 \frac{B}{B_\zeta R} + \mu B + Ze\tilde{\Phi}.$$

Here, P_ζ is the toroidal angular momentum, $\mu \equiv \frac{1}{2} M v_\perp^2 / B$ the magnetic moment, M the particle mass, B the magnetic field strength, Z the particle charge, $(\tilde{A}_\zeta, \tilde{\Phi})$ the perturbed (vector, scalar) potentials, ψ_p the poloidal magnetic flux, and R the major radius of the torus.

If $\ddot{\phi}/\dot{\phi}, \omega_b \ll \omega_\zeta, \omega_\theta$, a particle in the (n, m) resonance bucket has a bounce-averaged guiding center motion, caused by the frequency chirping, in (P_ζ, E, μ) space satisfying:

$$n\dot{\omega}_\zeta - m\dot{\omega}_\theta = \ddot{\phi}, \quad \text{motion of the bucket center;} \quad (4a)$$

$$\dot{P}_\zeta = \frac{n}{\phi} \dot{E}, \quad \text{a constraint near the } n\text{th resonance;} \quad (4b)$$

while μ is constant since $\dot{\phi} \ll \Omega$. Here, ω_b is the bounce frequency of particle trapped in the wave, and $\omega_\zeta(P_\zeta, E, \mu)$ and $\omega_\theta(P_\zeta, E, \mu)$ are bounce-averaged toroidal and poloidal angular rotational frequencies. More importantly, this motion in (P_ζ, E) space leads to a bounce-averaged radial motion governed by the toroidal force balance

$$\dot{\psi}_p = \frac{c}{Ze} \left(M \frac{d}{dt} \left\langle \frac{B_\zeta R}{B} v_\parallel \right\rangle - \dot{P}_\zeta \right), \quad (4c)$$

where $\langle \dots \rangle$ represents the bounce-average along the unperturbed orbit.

An explicit relation between the radial motion and the frequency chirping requires a calculation of $\omega_\zeta(P_\zeta, E, \mu)$ and $\omega_\theta(P_\zeta, E, \mu)$. For orbits with a finite width in general toroidal geometry, this is usually not possible, and a numerical study [11] is required. However, it is easy to see that a negative chirping, $\ddot{\phi} < 0$, typically leads to decreasing

P_ζ (thus decreasing energy) and consequently causes an outward radial drift, as shown in Fig. 3c. In addition, as the particle moves radially outward, its pitch angle decreases. For an originally well confined counter-circulating particle, the decrease of the pitch-angle can cause it to cross the trapped/passing boundary [8] and to turn into a fat banana, as shown in Fig. 3d. Note that Fig. 3 is obtained from deploying a chirped frequency wave and a D-shaped tokamak plasma equilibrium in the Hamiltonian guiding center orbit-following code [8,10,11]. For a more detailed studies of various types of chirped-frequency-induced convection and topological bifurcations, we refer the reader to Ref. [7]. Also note that the rate of the radial drift is not sensitive to the wave amplitude. However, as indicated in the 1-D model, to form a finite size bucket the ratio of wave amplitude to frequency change rate has to exceed a certain value.

By assuming large aspect ratio and neglecting finite orbit width effects, Eqs. (4a)-(4c) yield the following analytic expressions for the radial drift induced by frequency chirping:

$$\frac{\dot{r}}{r} \simeq -\frac{m}{k_{\parallel}^2 r^2} \frac{\ddot{\phi}}{\Omega} / \left(1 - \frac{mS}{k_{\parallel}^3 r^2 q R} \frac{\dot{\phi}}{\Omega} \right); \quad \text{well passing orbits} \quad (5a)$$

$$\frac{\dot{r}}{r} \simeq \frac{-\ddot{\phi}}{(1-S)\dot{\phi} + (2-3S)m\omega_\theta - \frac{m\omega_e^2}{8n\omega_c}}; \quad \text{deeply trapped orbit} \quad (5b)$$

where $\omega_\theta \simeq \sqrt{\frac{r}{2R}} \frac{v}{qR}$. Here, q is the safety factor, $S \equiv \frac{r}{q} \frac{d}{dr} q$ the magnetic shear, k_{\parallel} the parallel wave vector, and Ω the gyro-frequency.

When the poloidal bounce harmonic $m = 0$, as in *fishbone* oscillations, Eq. (5b) reduces to the simple relation $\frac{\dot{r}}{r} \simeq \frac{-\ddot{\phi}}{(1-S)\dot{\phi}}$. In other words, a frequency change of order unity leads to a change of radial position of order unity. In particular, by assuming $q = 1 + 2y$, one finds $\frac{y(1+2y_0)^2}{y_0(1+2y)^2} = \left(\frac{\omega_0}{\omega}\right)^2$, which indicates that in order to bring a deeply trapped particle originally captured by the bucket at $r_0 = a\sqrt{y_0}$ to the plasma edge ($r = a$), one needs to change the frequency from ω_0 to $\omega_f = \frac{3\sqrt{y_0}\omega_0}{1+2y_0}$ which has a minimum value at $y_0 = 0.5$. Here, $y \equiv \left(\frac{r}{a}\right)^2$, $y_0 = y(t = 0)$, and $\omega_0 = \omega(t = 0)$ is the initial wave frequency. This also implies that if $y_0 < 0.5$, one needs to first decrease the frequency from ω_0 to $\omega_1 = \frac{2\sqrt{2}}{3}\omega_f$ to bring the particle to $y_1 = 0.5$, and then to increase the frequency back to ω_f to bring particle to the plasma edge.

Similarly, for a well-circulating particle close to the $n = 1, m = 1$ bounce resonance, with $\omega_0/\Omega = 0.016$ (appropriate for Shear Alfvén modes induced by fusion alphas), Eq. (5a) yields $\left(1 - \frac{1}{1+2y}\right)^2 \dot{y} \simeq -0.32 \frac{\dot{\omega}}{\omega_0}$. Thus, to bring the particle from the center to the plasma edge requires $\frac{\omega_0}{\omega_f} \leq 4$. Note that the higher order term in the denominator of Eq. (5a) involving $S\dot{\phi}/\Omega$ has been neglected here for simplicity. However, if there exists a rational surface where $k_{\parallel} = 0$, this term becomes dominant and results in $\dot{r} = 0$. This is simply due to the fact that the particle can not be resonant with the wave at this rational surface unless the wave frequency also vanishes. One way to smoothly get across this surface is to keep decreasing the frequency from positive to negative.

The radial particle convection induced by frequency chirping can be large. It can be estimated by $N\sqrt{\frac{\delta B}{B_0}}\dot{r}$, where N is particle density, and δB the perturbed magnetic field. If $\frac{\delta B}{B_0} \simeq 10^{-4}$, $\frac{\dot{\omega}}{\omega_0^2} \simeq 10^{-3}$, and $\omega_0 \simeq 10^6 s^{-1}$, the radial flux is equivalent to that of diffusion with the diffusion coefficient $D \simeq 10m^2/s$. Still, for energetic particles with large orbit width, this is usually an underestimate. In particular, recall that a counter-circulating orbit can get across the trapped/passing boundary and turn into a fat banana in a wave with negative chirping, as shown in Fig. 3d. In addition, when untrapped particles are approached by the bucket, the amplitude of orbit oscillations in phase space increases. This enhances the near-boundary loss [8].

In summary, particle dynamics in chirped waves has been studied in both a 1-D system and a toroidally confined plasma system. It is demonstrated that a **convecting bucket** is formed, which traps particles within it and gives resonant kicks to untrapped particles when it collides with them in phase space. In toroidal systems, this leads to a radial convection. Analytic expressions for the radial flow induced by frequency chirping are obtained in the thin orbit width and large aspect ratio limit. A more detailed discussions will be given elsewhere [7], and more complicated features such as bucket dynamics in the presence of orbit stochasticity, are subject to future investigation. There are many potential applications of this mechanism since frequency chirping is a common feature of nonlinear systems. In particular, a radial standing wave propagating in a magnetic surface of a tokamak inevitably undergoes nonlinear evolution accompanied by a continuous frequency shift before it saturates [12].

It appears worth while to investigate the additional anomalous transport fluxes of hot ions induced by frequency chirping in toroidally confined plasmas. Previous such studies have mostly relied on stochastic quasilinear diffusion [8] which requires the amplitude of fluctuations to exceed the stochastic threshold. A recent experimental investigation [13] of energetic particle losses in tokamaks during beam driven instabilities such as *fishbones* [2] and/or Toroidal Alfvén Eigenmodes [13,14] has shown that (1) there is no clear sign of an amplitude threshold for the losses to occur, and (2) the loss flux appears dominated by convection. The present mechanism can potentially lead to considerable anomalous radial convection without an amplitude threshold, and may thus contribute importantly to the observed transport fluxes.

By launching controllable electromagnetic waves with chirped frequency, the present mechanism may be utilized to selectively redistribute charged particles radially in tokamak plasmas. This mechanism may thus possibly be used (i) to pump out unwanted fusion ashes or impurities to avoid fuel dilution; (ii) to inject energetic fuel ions into the plasma core for continuous controlled fueling; and (iii) to move groups of locally produced particles away from particular radial resonance location to avoid certain instabilities. The applicability and efficiency of these processes, which are obviously very sensitive to the properties of wave to be excited in the plasma, are under investigation by the authors.

Acknowledgement

One the authors (CTH) would like to thank Drs. C.P. Chen and S.C. Chen of MIT for many fruitful discussions and suggestions. This work was supported by the U.S. Department of Energy under Grant No. DEFG02-91ER-54109 and partially supported by the Royal Swedish Academy of Sciences.

Figure Captions

- ¹ Potential and phase space trajectories in the wave frame with constant frequency chirping $\ddot{\phi}$: (a), Potential $V(Q)$ vs Q ; and (b), Contours of constant $\hat{H}(P, Q)$.
- ² Momentum p vs time in a 1-D Hamiltonian system with finite frequency chirping $\ddot{\phi}$: (a) for a particle trapped in the bucket with constant $\ddot{\phi}$; (b) for an untrapped particle kicked by the bucket with constant $\ddot{\phi}$; (c) for a particle trapped in the bucket with $\phi(t) = t \exp(-t/20)$.
- ³ Orbit drift due to chirped-frequency wave in an axisymmetric toroidal plasma: (a) normalized frequency $\dot{\phi}R_0/v_0$ vs $\hat{T} \equiv v_0 t/2\pi R_0$, where R_0 the major radius, and v_0 the initial particle velocity; (b) change of toroidal angular momentum $P_\zeta(t) - P_\zeta(0)$ vs \hat{T} ; (c) trajectory of a co-going orbit trapped in the bucket; (d) trajectory of a counter-going orbit which changes its pitch-angle in the bucket and finally turns into a fat banana.

References

- [1] D. Marcuse, *Applied Optics* **20**, 3573 (1981).
- [2] M.F.F Nave, et al., *Nuclear Fusion* **31**, 697 (1991).
- [3] J.L. Tennyson, J.R. Cary, and D.F. Escande, *Phys. Rev. Lett.* **56**, 2117 (1986); A.I. Neishtadt, *Sov. J. Plasma Phys.* **12**, 568 (1986) [*Fiz. Plazmy* **12**, 992 (1986)].
- [4] N.M. Kroll, P.L. Morton, and M.N. Rosenbluth, *Physics of Quantum Electronics*, (Addison-Wesley, Reading Massachusetts, 1978), Vol. 7, Chap. 4.
- [5] P. Helander, M. Lisak, and V.E. Semenov, *Phys. Rev. Lett.* **68**, 3659 (1992).
- [6] A.J. Lichtenberg and M.A. Lieberman, *Regular and Stochastic Motion*, (Springer-Verlag, New York, 1983).
- [7] C.T. Hsu, P. Helander, and C.Z. Cheng, (in preparation).
- [8] C.T. Hsu, D.J. Sigmar, *Phys. Fluids* **B4**, 1492 (1992).
- [9] B.V. Chirikov, *Phys. Reports* **52**, 265 (1979).

- [10] R.B. White, M.S. Chance, *Phys. Fluids* **27**, 2455 (1984).
- [11] C.T. Hsu, D.J. Sigmar, B.N. Breizman, # 3C37, Sherwood Theory Conference, Newport, Rhode Island, (1993); also in preparation for submission to *Phys. Fluids*.
- [12] F.Y. Gang, (private communication).
- [13] W.W. Heidbrink, et al., *Phys. Fluids* **B5**, 2176 (1993).
- [14] K.L. Wong, et al., *Phys. Rev. Lett.* **66**, 1874 (1991); C.Z. Cheng, M.S. Chance, *Phys. Fluids* **29**, 3695 (1985).

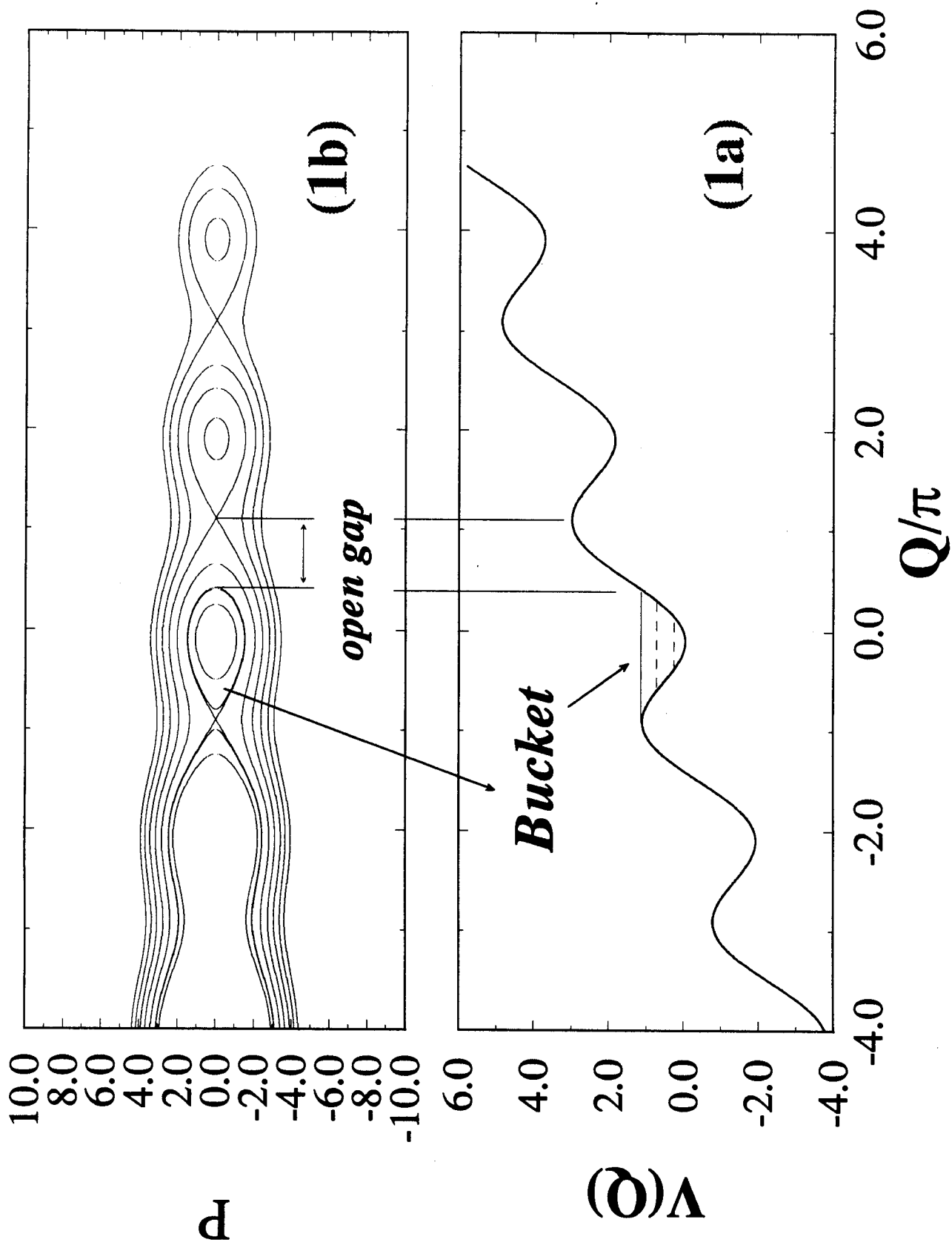


Fig. 1

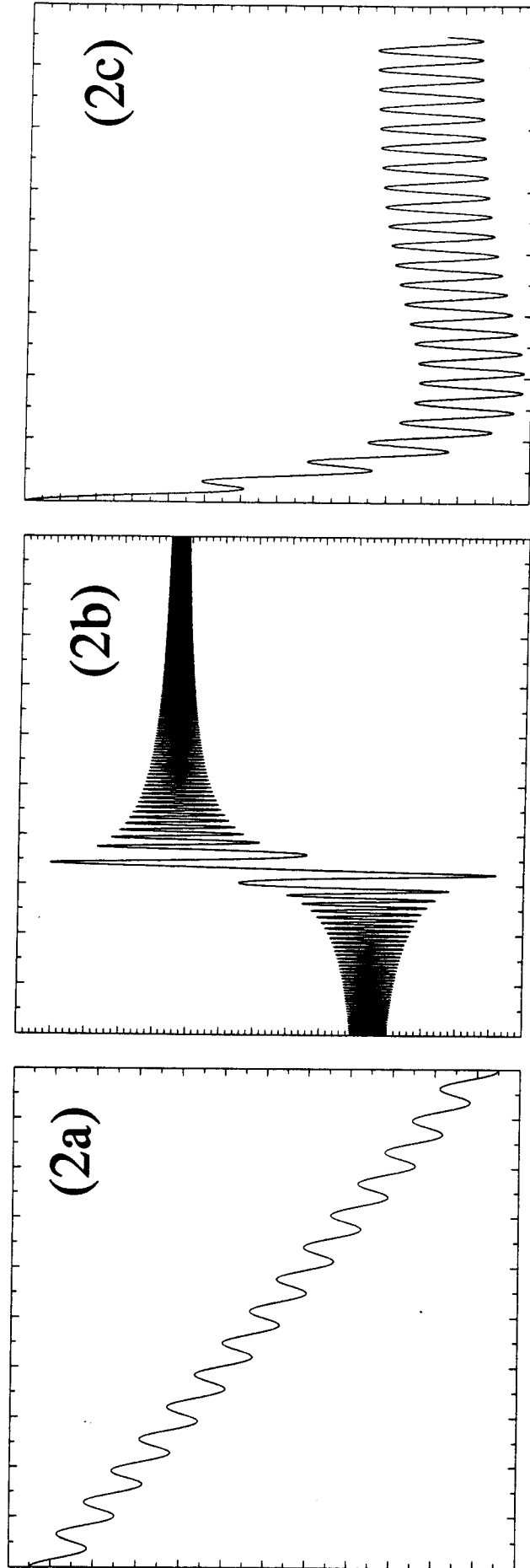


Fig. 2

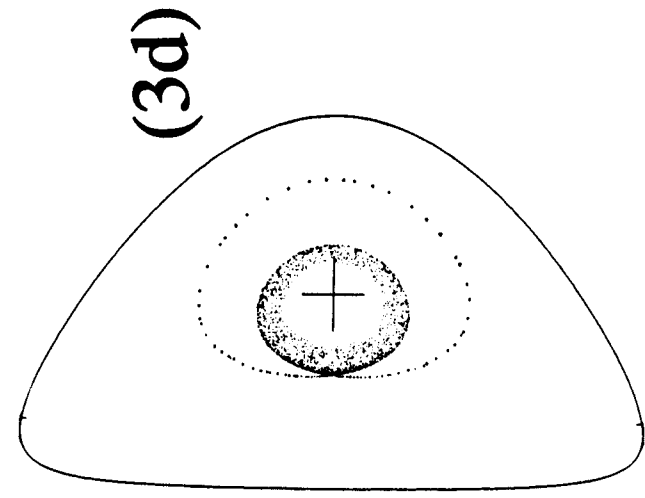
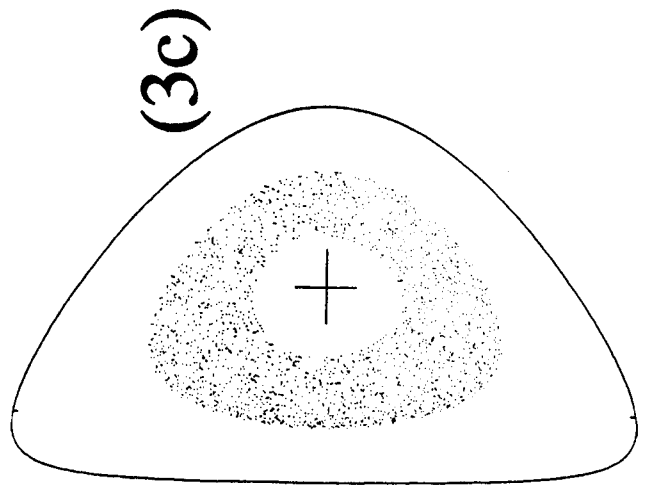
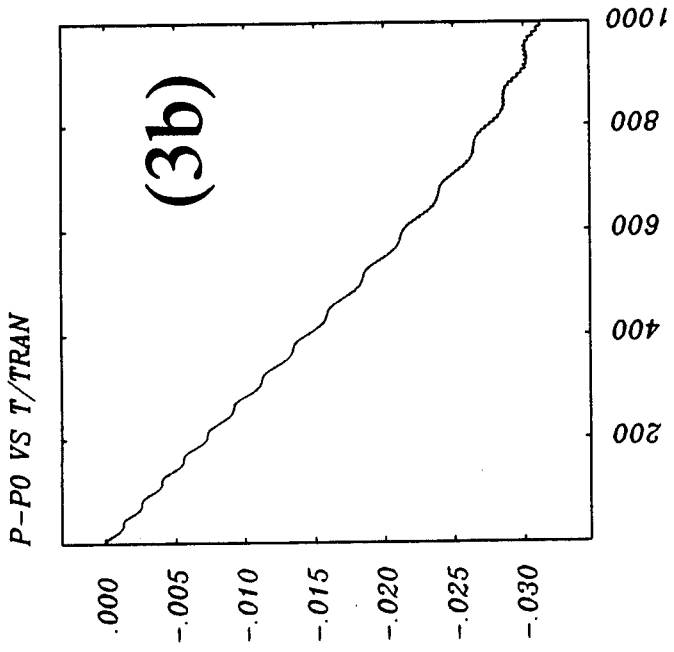
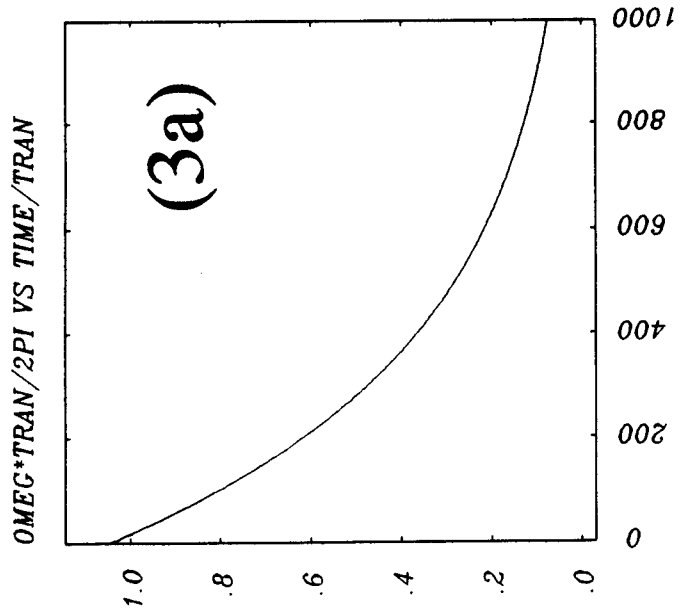


Fig. 3